Development 133, 2233-2241 (2006) doi:10.1242/dev.02378

A β1,4-galactosyltransferase is required for Bmp2-dependent patterning of the dorsoventral axis during zebrafish embryogenesis

Quentin J. Machingo[1], Andreas Fritz[2] and Barry D. Shur[1,*]

Complex carbohydrates are highly polymorphic macromolecules that are involved in diverse biological processes; however, a detailed understanding of their function remains obscure. To better define the roles of complex carbohydrates during vertebrate embryogenesis, we have initiated an analysis of glycosyltransferase function using the zebrafish system. In this study, we report the characterization of a zebrafish β1,4-galactosyltransferase (GalT), which has substantial homology with mammalian β4GalT5 and is expressed zygotically throughout the zebrafish embryo. Downregulating the expression of β4GalT5 by injection of specific morpholino oligonucleotides results in dorsalized zebrafish embryos, suggesting a role of β4GalT5 in Bmp2-mediated specification of the dorsoventral axis. Consistent with this, morpholino-injected embryos have ventrally expanded chordin expression and reduced activation of the Bmp-dependent transcription factors Smad1/5/8. Because other growth factors, such as Egf and Fgf, require binding to extracellular proteoglycans for delivery and/or binding to their cognate receptors, we examined whether proteoglycans isolated from control and morpholino-injected embryos show differential binding affinities for Bmp2. In this regard, proteoglycans isolated from β4GalT5 morphant embryos are underglycosylated and are unable to bind recombinant Bmp2 as efficiently as proteoglycans from control-injected embryos, whereas the binding of Bmp7 is relatively unaffected. These results suggest that β4GalT5 is a previously unidentified zebrafish galactosyltransferase that is essential for proper patterning of the dorsoventral axis by regulating Bmp2 signaling. Furthermore, this work demonstrates that a relatively simple carbohydrate modification to endogenous proteoglycans can modulate the specificity of cytokine signaling.

KEY WORDS: Galactosyltransferase, Bmp, Zebrafish, Embryonic axis

INTRODUCTION

Complex carbohydrates are widespread throughout cells and tissues, and are predominant components of the extracellular matrix and the cell surface. The enormous diversity of complex carbohydrate structures results from the concerted action of specific glycosyltransferases and associated enzymes involved in carbohydrate synthesis. Given the ubiquitous expression of complex carbohydrates and their biosynthetic enzymes, it is likely that they play many different roles within the organism (Varki, 1993). However, the complexity of carbohydrate structures and of their biosynthetic enzymes has made it difficult to define their function in vivo, particularly during vertebrate embryogenesis.

Most studies of complex carbohydrate function during vertebrate development have relied upon the characterization of targeted knockouts of specific glycosyltransferases of interest. This approach has yielded important clues about the overall requirement of *N*-linked glycoside chains during early development, and about the role of specific monosaccharide residues in various physiological events (Domino et al., 2001; Ioffe and Stanley, 1994; Lu et al., 1997; Maly et al., 1996). Furthermore, and perhaps more importantly, these studies have shown that glycosyltransferases are a much more polymorphic class of enzymes than previously thought. For example, targeted deletion of β1,4-galactosyltransferase uncovered the existence of five additional genes that encode β1,4-galactosyltransferases. In light of the large number of individual glycosyltransferases thought to be active in mammalian tissues (e.g. ~150-300), it becomes difficult to achieve a more global understanding of carbohydrate function through traditional knockout approaches. To address this limitation, we have taken advantage of the zebrafish system, which is more amenable to a high throughput analysis, to investigate the function of glycosyltransferases during development. Herein, we describe an essential and unexpected role for a β1,4-galactosyltransferase in patterning of the early embryo by participating in proteoglycan glycosylation that is required for Bmp-dependent specification of the dorsoventral axis.

[1]Department of Cell Biology, Emory University School of Medicine, 615 Michael Street, Atlanta, GA 30322, USA. [2]Department of Biology, Emory University, 1510 Clifton Road, Atlanta, GA 30322, USA.

*Author for correspondence (e-mail: barry@cellbio.emory.edu)

Accepted 28 March 2006

MATERIALS AND METHODS

Fish

Zebrafish, *Danio rerio*, were maintained at 28°C as described previously (Westerfield, 1993). All experiments were performed using random matings of *AB animals. Embryos were collected, raised and staged in embryo medium until they reached the desired developmental stage. Developmental stage was determined following previously defined criteria (Kimmel et al., 1995). Allele designations for zebrafish mutants used in this study include: *pgy* (*piggytail*), *snh* (*snailhouse*) and *swr* (*swirl*) (Mullins et al., 1996).

In silico identification of β4-galactosyltransferases

Putative zebrafish β4-galactosyltransferases (β4GalTs) were identified through searches of the zebrafish genomic database (Sanger Institute). Briefly, mammalian β4GalTs (human β4GalT5, NM_004776 and mouse β4GalT5, NM_019835) were used as query sequences. Putative trace sequences were merged into contigs using the Lasergene sequence management software (DNASTAR) to determine the full-length sequences. Identified sequences were BLASTed against the genome assembly to identify putative splice sites. Primary amino acid sequence, as well as genetic structure, was used to define homology. Simple phylogeny was determined based upon parsimony, aligning the known human β4GalTs

(NM_001497, NM_003780, NM_003779, NM_212543, NM_004775) with putative zebrafish orthologs using protpars (J. Felsenstein, unpublished). An unrooted phylogenetic tree was inferred from the alignment using megalign (DNASTAR) and ClusalW (Thompson et al., 1994).

Cloning of full-length zebrafish β4GalT5

β4GalT5 was cloned by RT-PCR from total RNA isolated from 72-hour zebrafish embryos. Primers (Operon) were designed to the central region of β4GalT5 and used to amplify a core fragment. Additional primers within the core fragment were used to perform both 5′ and 3′ RACE. The RACE fragments were gel purified and overlapping regions between the 5′ RACE, the core fragment and the 3′ RACE were annealed. The full-length transcript was generated by PCR using primers designed to the 5′ and 3′ UTR. The full-length transcript was then cloned into pCRII (Invitrogen). Full-length β4GalT5 was subjected to site-directed mutagenesis to introduce silent mutations into the morpholino recognition site that would eliminate binding (Gene-Tailor, Invitrogen). The MO3 recognition sequence (TAATGCCGA-CACATCTGAGA) was modified to TTATGCCCACACACCTAAGC.

Whole-mount in situ hybridization

Whole-mount in situ hybridization was performed as described previously (Thisse and Thisse, 1998). Briefly, staged embryos were fixed in 4% paraformaldehyde and dehydrated in methanol. Following rehydration into phosphate-buffered saline/0.1% Tween-20, embryos were prehybridized for 1 hour at 65°C. Hybridization with gene-specific probes was conducted overnight at 65°C. DIG-labeled probes were detected with α-DIG antibodies (Roche) and visualized with BCIP/NBT (Vector Labs). Plasmids containing *chordin* were kindly provided by M. Halpern (Carnegie Institution). *pax2a*, *mkp3* and *β4galt5* RNA antisense probes were synthesized with T7 from *Bam*H1 linearized plasmids. Sense controls were generated from *Not*1 linearized plasmids and transcribed with Sp6. At least 10 embryos were used in each assay. All in situ hybridizations were repeated at least three times.

Microinjection of morpholino oligonucleotides and full-length RNA

Antisense morpholino oligonucleotides were designed to compliment either a sequence in the 5′UTR of β4GalT5 (MO1, 5′-CACTGCTGGAAATGT-AAATACTCAT-3′; base pairs –245 to –221), an internal splice site of β4GalT5 (MO2, 5′-ACGTGAACCCTGTCGCGTCCTGTCA-3′; base pairs +176 to +186 plus 15 intronic base pairs) or the start codon of β4GalT5 (MO3, 5′-CGAAATCTCAGATGTGTCGGCATTA-3′; base pairs –2 to +23) (Gene-Tools). Morpholinos were resuspended in 1×Daneau Buffer prior to injection (Nasevicius and Ekker, 2000). Various concentrations, as described in the text, were injected into the cytoplasmic stream of two- and four-cell embryos. Morpholinos to other galactosyltransferases or an irrelevant morpholino oligonucleotide (5′-CCTCTTACCTCAGTTACAA-TTTATA-3′) were injected as controls. Full-length transcripts of β4GalT5 and mutated β4GalT5 were subcloned into the pCRII plasmid (Invitrogen). Mature capped and poly-adenylated mRNA was transcribed from *Bam*H1 linearized plasmids using the T7 or Sp6 mMessage mMachine kit (Ambion). mRNA was diluted in water and various concentrations were injected into the cytoplasmic stream of two- and four-cell embryos. Antisense mRNA at the same concentrations was injected as a control.

Western blot analysis

Embryos were lyzed in ice-cold lysis buffer (0.5% Triton X-100, 150 mM NaCl, 20 nM Tris-HCl, 10 mM EDTA) and electrophoresed on 7.5% SDS-PAGE for α-Smad blots. Fifteen percent SDS-PAGE gels were used for α-Bmp blotting. Blots were transferred to PVDF (Millipore) membranes and blocked in 5% nonfat dry milk in 20 mM Tris-HCl, 150 mM NaCl (TBS) plus 0.1% Tween-20 (TBST) for 1 hour at room temperature. Following block, membranes were incubated in primary antibody (α-Smad5, 1:1000, Cell Signaling; α-phospho-Smad1/5/8, 1:1000, Cell Signaling; α-Bmp2, 2 μg/ml, Sigma; or α-Bmp7, 2 μg/ml, Alpha Diagnostic International) in 5% BSA in TBST for 12 hours at 4°C. Following three washes in TBST, membranes were incubated in secondary antibody [goat α-rabbit-HRP (Santa Cruz) or α-mouse-HRP (Santa Cruz), both at 1:25,000 dilutions] in 5% BSA in TBST for 1 hour at room temperature. Following three washes in TBST and two washes in TBS, antibody reactivity was detected using ECL detection (Amersham).

Proteoglycan isolation and Bmp-binding assay

Proteoglycans were extracted as described previously from deyolked 85% epiboly embryos (Hascall and Kimura, 1982). Briefly, embryos were placed in ice-cold 4 M guanidine-HCl, 0.2% w/v zwittergent 3-12, 50 mM sodium acetate, 10 mM EDTA with protease inhibitors (Roche), and incubated at 4°C for 1 hour. The lysates were cleared by spinning at 15,000× ***g*** for 10 minutes at 4°C. The supernatant was removed and dialyzed against 20 mM Tris-HCl, pH 7.4, for 18 hours at 4°C. The proteoglycans were precipitated using 5% cetylpyridinium chloride at 37°C for 1 hour. The precipitate was washed in 0.5 M sodium acetate/95% ethanol followed by 0.5 M sodium acetate/10% ethanol. The final pellet was resuspended in 20 mM HEPES, pH 7.4. For SDS-PAGE of isolated proteoglycans, samples were run on a 5% polyacrylamide gel. The gel was fixed in 50% methanol/5% acetic acid for 1 hour and washed in 3% acetic acid for 20 minutes with one change of the wash solution. Carbohydrates were oxidized for 30 minutes with 10 mg/ml periodic acid in 3% acetic acid. The gel was again washed for 20 minutes with 3% acetic acid and stained with Pro-Q emerald (Molecular Probes) for 2 hours and visualized at 300 nm. The gel was then stained for total protein by incubating with SYPRO stain (Molecular Probes) and visualized at 300 nm.

For affinity chromatography, 100 μl of purified proteoglycans were coupled to an Affi-Gel 10 (BioRad) column. Briefly, 100 μl Affi-Gel 10 was washed with distilled water. Purified proteoglycans were added to the matrix, and incubated at room temperature for 1 hour. Following ligand binding, unbound sites were blocked with 0.1 M ethanolamine-HCl, pH 8, for 1 hour at room temperature. The bound and blocked matrix was added to a 1 ml syringe filled with approximately 100 μl volume of glass wool. The column was washed with 3 ml HEPES, pH 7.4 and stored at 4°C. All liquids were applied to the column and allowed to flow by gravity. Prior to use, the columns were washed with 1 ml 20 mM Tris-HCl, pH 7.4. Recombinant human BMP2 (Sigma) or recombinant human BMP7 (Sigma) (2 μg) was applied to the columns and allowed to bind. Following binding, the columns were washed with 1 ml 20 mM Tris-HCl, pH 7.4, and the BMP was eluted with increasing concentrations of NaCl in 20 mM Tris-HCl, pH 7.4. Fractionated eluent was separated by SDS-PAGE and probed for BMP2 or BMP7 by western blotting, as described above.

RESULTS

Cloning of a zebrafish *β4GalT5*

The zebrafish EST and genomic sequence databases were queried for sequences that are similar to mammalian β4GalTs. One transcript identified had 69.9% identity at the amino acid level to the human β4GalT5 (Fig. 1A) and was designated β4galt5 (Accession number DQ104219). The zebrafish β4galt5 transcript is predicted to contain nine exons (Fig. 1B), and retains the genomic structure predicted for human β4GalT5. mRNA transcribed from the zebrafish *β4galt5* gene is 1,143 base pairs in length and encodes a 382 amino acid protein. The zebrafish sequence contains conserved motifs that are thought to be essential for sugar-nucleotide binding, including the FNRA, DVD and WGWG(G)EDDD motifs (Hagen et al., 1999). A simple phylogenetic analysis (Fig. 1C) reveals that zebrafish β4GalT5 is ancestral to a subgroup of the β4GalT family that includes the β4GalT5s and the β4GalT6s.

β4galt5 is expressed throughout the embryo following initiation of zygotic transcription

To define the temporal expression of *β4galt5*, semi-quantitative RT-PCR was preformed with staged RNA libraries (Fig. 2A). In the oocyte, high levels of control mRNA [*brul*, a maternally and zygotically expressed RNA-binding protein (Suzuki et al., 2000)] were detected (data not shown); however, there was no detectable expression of *β4galt5*. Low levels of β4galt5 were first evident at 50% epiboly and reached peak expression by the 12-somite stage. Levels of β4GalT5 remained consistently high in Prim-16 stage embryos. Thus, β4GalT5 is not maternally loaded into the oocyte and peak expression is reached by mid-somitogenesis.

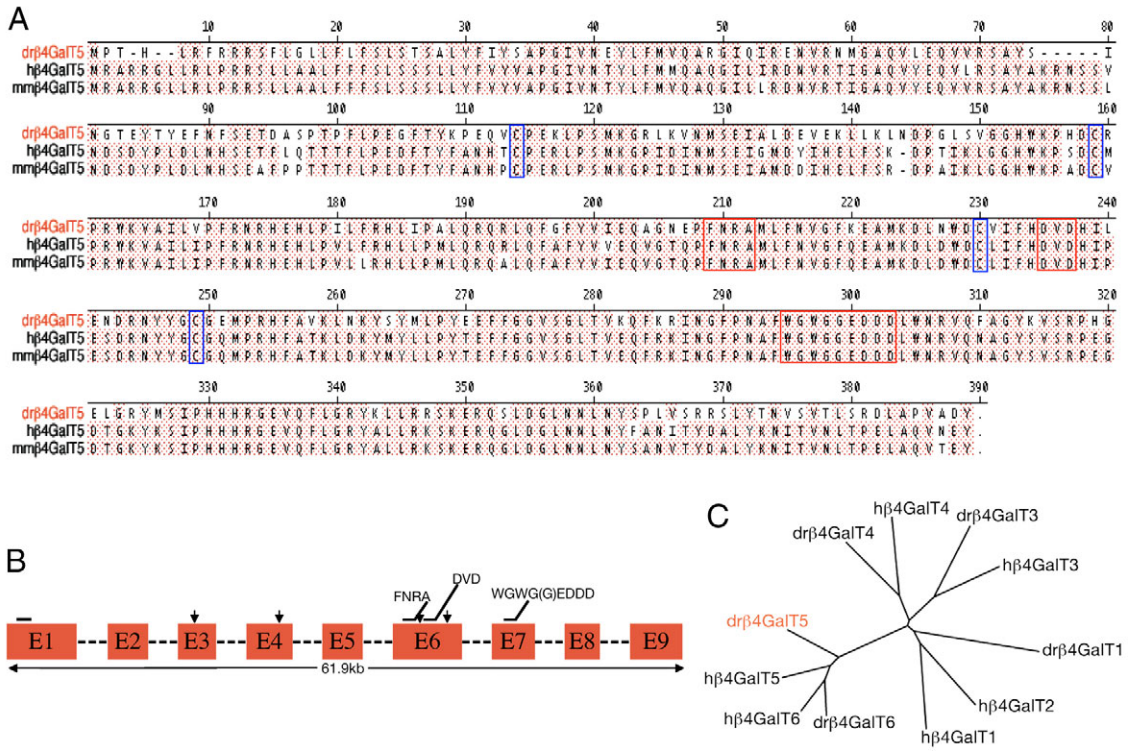

Fig. 1. Sequence alignment, genetic structure and family homology of putative zebrafish β4GalT5. (**A**) Sequence alignment of zebrafish, human and mouse β4GalT5 proteins. Identical sequences are shaded in red. Conserved cysteines used to align sequences are boxed in blue and predicted sugar-nucleotide binding sites are boxed in red. (**B**) Predicted gene structure of *β4galt5*. Exons are boxed, introns indicated by dashed lines. Arrows indicate conserved cysteines and the solid line above exon 1 indicates the predicted signal sequence and transmembrane domain; sugar-nucleotide binding motifs are also indicated (Lo et al., 1998). (**C**) Unrooted phylogenetic tree of human (h) and zebrafish (dr) β4GalTs (drβ4GalT5, red).

To address the spatial localization of β4GalT5, whole-mount in situ hybridization was performed. Low expression was first detectable in 50% epiboly embryos (Fig. 2B) and was uniform throughout the embryo. Occasionally, slightly higher levels of expression were seen in the hypoblast along the primary embryonic axis (arrow, Fig. 2B), although this may reflect increased tissue mass along the axis. During early somitogenesis (bud stage; Fig. 2C), β4GalT5 was expressed uniformly throughout the embryo, including expression in the polster. Later in somitogenesis (12 somites, Fig. 2D), expression was elevated in the ventral regions of the embryo, as well as at the midline (arrow, Fig. 2D). By the 26-somite stage, it was possible to identify specific structures with noticeably higher levels of β4GalT5, such as in the

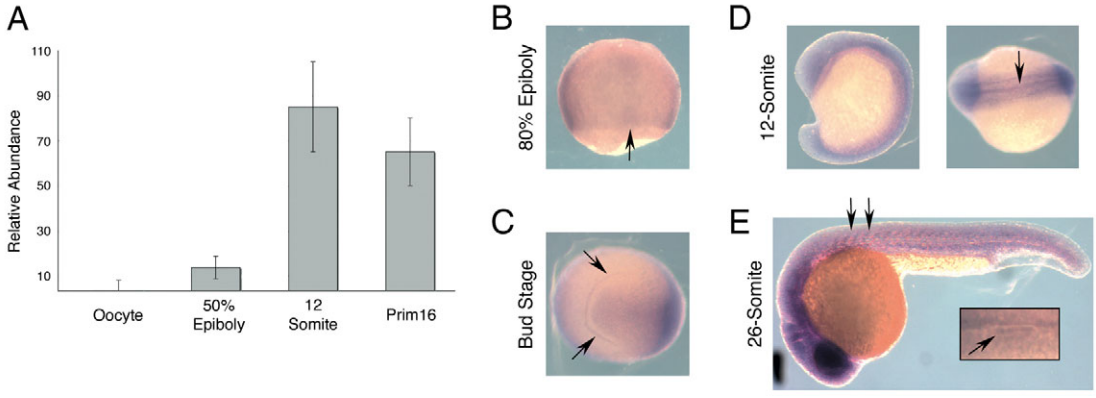

Fig. 2. Temporal and spatial expression of *β4galt5* during zebrafish embryogenesis. (**A**) RT-PCR analysis of staged RNA provides a temporal profile of *β4galt5* expression. There was no detectable level of β4GalT5 in oocytes. Expression was first detected in the early gastrula embryo (50% epiboly), and reached a steady state by mid-somitogenesis. Error bars indicate s.e.m. (**B-E**) Whole-mount in situ hybridization of *β4galt5*. Expression is widespread throughout the embryo with some refinement in stage-specific structures. (B) Dorsal view of 80% epiboly embryo. Note expression throughout the embryo with a slight increase in the dorsal axis (arrow); peripheral stain reflects 'edge effects' due to oocyte curvature. (C,D) Near ubiquitous expression throughout the bud (C, anterior view) and 12-somite stage embryo (D, lateral view, dorsal view at hindbrain level). Note expression in the developing polster (arrows, C) and floorplate (arrow, D). (E) Twenty-six-somite stage embryos (lateral view). Arrows indicate higher expression in intersomitic boundary. Inset illustrates expression at the midline of the otic vesicle (arrow).

Table 1. Dorsalization phenotype of β4GalT5 morphant embryos and mRNA rescue

	Wild type	Class 3* – mild dorsalization (similar to *pgy*)	Class 4* – moderate dorsalization (similar to *snh*)	Class 5* – severe dorsalization (similar to *swr*)	Percent displaying phenotype
5 ng MO1 (*n*=57†)	14% (8‡)	72% (41)	14% (8)	0	86% (49)
10 ng MO1 (*n*=373)	15% (55)	13% (50)	60% (223)	12% (45)	85% (318)
20 ng MO1 (*n*=78)	15% (12)	5% (4)	14% (11)	65% (51)	85% (66)
10 ng MO2 (*n*=324)	19% (61)	13% (42)	38% (122)	31% (99)	81% (263)
10 ng MO3 (*n*=111)	19% (21)	19% (21)	28% (31)	34% (38)	82% (90)
10 ng MO3 + 40 pg mdrβ4GalT5 mRNA (*n*=118)	71% (84)	3% (3)	14% (17)	14% (16)	31% (36)

*Classified according to Mullins et al. (Mullins et al., 1996).
†Total embryos treated.
‡Total embryos in each class.
MO1, translation blocker (–50 bp); MO2, splice blocker (exon 1 splice donor); MO3, translation blocker (start site); mdrβ4GalT5 mRNA, MO3-binding site abolished.

intersomitic spaces of the trunk (arrows, Fig. 2E), as well as in the otic vesicle (insert, Fig. 2E). Parallel incubations using the sense β4GalT5 probe produced no detectable signal.

Knockdown of β4GalT5 results in severe dorsalization

The widespread expression of β4GalT5 makes it difficult to predict its developmental role. To address its function in vivo, morpholino oligonucleotides specific to β4GalT5 were injected into two- and four-cell embryos. A total of three independent morpholinos were used: two different translation blocking morpholinos (MO1, MO3) and one splice blocking morpholino (MO2); all injected morpholinos produced nearly identical phenotypes (Table 1), and all subsequent studies were repeated with at least two independent morpholinos. For controls, ~20 embryos were injected in each experiment with equal amounts of an irrelevant morpholino. The degree of embryonic death was similar (<10% death) in all injections, irrelevant of the morpholino injected. However, developmental defects were only seen in embryos injected with β4GalT5-specific morpholinos; all surviving embryos injected with control morpholinos appeared normal (Fig. 3B).

The earliest phenotype detectable in morpholino-injected embryos was evident at 80% epiboly as an exaggerated elongation of the embryo. By the 2-somite stage, morpholino-injected embryos were clearly elongated and displayed a defective tail bud (Fig. 3A). Extensive coiling of the tail and other indicators of dorsalization were seen when control embryos had reached the 26-somite stage, at which time three classes of morphant phenotypes of increasing severity were observed.

The β4GalT5 morphant phenotypes were classified according to the criteria defined by Mullins et al. (Mullins et al., 1996) for dorsoventral defects. The three classes of β4GalT5 morphants roughly correspond to the three most severe classes of dorsoventral phenotypes described by Mullins et al. (Mullins et al., 1996). Class 3 embryos are similar to the *pgy* mutant (Fig. 3C), in that they have a slightly coiled tail indicative of mild dorsalization, and display moderate ear defects, including small otic fields and an absence of otoliths (asterisk, Fig. 3E). Interestingly, both wild-type and β4GalT5MO embryos express *pax2a*, a marker of the otic vesicle (Pfeffer et al., 1998); however, the *pax2a* field in β4GalT5MO embryos is smaller and rounder than in wild-type embryos (Fig. 3E).

Class 4 embryos are similar to the *snh* mutant and display a more significant coiling of the tail, as well as dorsalization within the anterior regions of the embryo, and are considered moderately dorsalized (Fig. 3C). Due to the severity of the phenotype, no otic structures were detected in this class of morphants, although both Class 4 and Class 5 embryos, in our hands, have *pax2a* staining in a region that is consistent with the otic field (data not shown). Class 5 embryos, similar to *swr* mutants (Fig. 3C), are the most severely affected and display a completely dorsalized phenotype.

The penetrance of the morpholino phenotype was directly dependent upon the amount of β4GalT5 morpholino injected. As demonstrated for β4GalT5MO1 (Table 1), injection of 5 ng morpholino resulted in a greater proportion of Class 3 embryos and few Class 5 embryos; whereas 20 ng resulted in high proportions of Class 5 embryos and few Class 3 embryos. Thus, the severity of the β4GalT5 morpholino phenotype was dose dependent.

Whereas the use of multiple independent morpholino oligonucleotides is taken as evidence that the phenotype results from downregulating the target (i.e. β4GalT5) transcript (Nechiporuk et al., 2005; Yan et al., 2005), we tested the specificity of the β4GalT5 morpholinos by injection of mRNA encoding full-length β4GalT5 in combination with β4GalT5MO3 (Table 1). Injection of 40 pg full-length mRNA in combination with 10 ng morpholino resulted in a rescue of the β4GalT5 knockdown phenotype, i.e. a wild-type appearance (Fig. 3D). Injection of full-length β4GalT5 mRNA in the absence of morpholino did not produce any noticeable phenotype. These results demonstrate that the phenotype observed following injection of β4GalT5 morpholino oligonucleotides results from a specific reduction of β4GalT5.

Because the β4GalT5MO phenotype grossly phenocopies the *swr*, *snh* and *sbn* mutations, which are characterized by dorsalized embryos resulting from mutations in *bmp2b*, *bmp7* or *smad5*, respectively (Dick et al., 2000; Hild et al., 1999; Kishimoto et al., 1997), it was important to determine whether downregulating β4GalT5 had a synergistic effect with these mutations. Knockdown of β4GalT5 in *swr* (*bmp2b*) mutants failed to reveal any additional phenotype, which may simply reflect the pre-existing severely dorsalized phenotype in *swr* mutants. However, knockdown of β4GalT5 accentuated the moderate phenotype of *snh* (*bmp7*) mutants into a more severe dorsalized appearance, similar to that seen in the *swr* mutant (22 out of 24 morpholino-injected embryos showed a *swr* phenotype versus 0 out of 24 control-injected embryos). The failure of β4GalT5 knockdown to influence the *swr* phenotype and to increase the dorsalization of the more moderate *snh* mutant is consistent with a β4GalT5 function in Bmp signaling.

chordin expression is unrestricted in β4GalT5 morphant embryos

Bmp2b and Bmp7 generate a negative-feedback loop with chordin that is required for the proper establishment of the dorsoventral margin. In mutants with defective Bmp signaling, such as *swr* and

snh, chordin expression invades the ventral hemisphere, a result of relieving the Bmp inhibition (Miller-Bertoglio et al., 1997). Therefore, we examined *chordin* expression in 85% epiboly embryos by in situ hybridization to determine whether Bmp signaling is altered following β4GalT5 knockdown. As reported, *chordin* expression was high in the dorsal axis of control-injected embryos (Fig. 4A; asterisk indicates dorsal axis in all panels) and restricted from the ventral hemisphere (arrows, Fig. 4A). β4GalT5MO embryos had no obvious dorsal axis when viewed dorsally (Fig. 4B); however, the axis was evident in the animal view (Fig. 4B). Moreover, *chordin* expression was expanded both ventrally and anteriorly (Fig. 4B). The expanded *chordin* expression in the presumptive ventral domain was also apparent when viewed from the vegetal pole (Fig. 4B), where *chordin* expression had completely enveloped the ventral hemisphere.

Because dorsalization is a common side effect of morpholino injection, we assayed the expression of other signaling pathways that participate during dorsoventral axis patterning. Of these, the Fgf signaling pathway is a crucial component underlying dorsoventral patterning, and, consequently, we examined the expression of *mkp3*, a downstream mediator of Fgf signaling (Tsang et al., 2004). As shown in Fig. 4, *mkp3* expression is unaltered in the β4GalT5 morphant background, being localized to the dorsal axis in both control-injected and β4GalT5 morphants (arrowheads). Similarly, we determined that the specification and/or patterning of dorsal structures appears grossly normal in β4GalT5MO embryos, as assayed by in situ hybridization of the dorsal markers *ntl* and *pax2* (data not shown). Collectively, all of the morphological and molecular characterization of the β4GalT5MO phenotype is indicative of disrupted Bmp signaling, and, consequently, Bmp signaling was assayed directly in β4GalT5MO embryos.

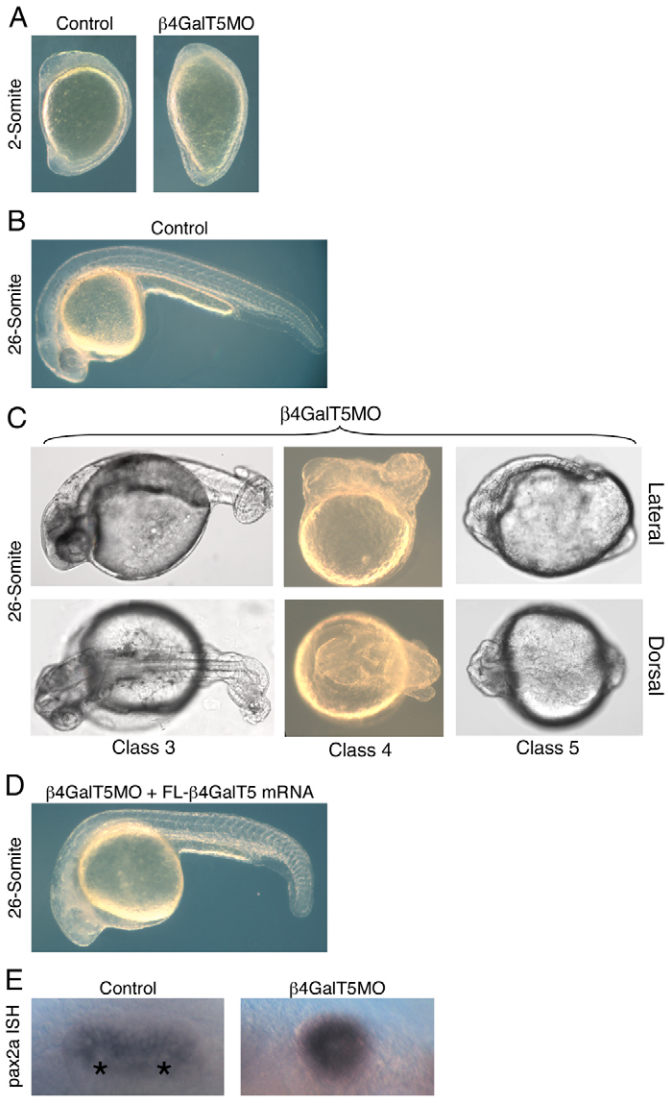

Fig. 3. Knockdown of β4GalT5 results in dorsalization. (**A**) Lateral views of 2-somite control-injected and β4GalT5MO-injected embryos. The morphant phenotype is manifested by an elongation of the anteroposterior axis. (**B**) 26-somite embryo injected with control morpholinos, lateral view. (**C**) When β4GalT5MO-injected embryos reach the 26-somite stage, the mature β4GalT5MO phenotype is observed (lateral and dorsal views). (Class 3) 5 ng of β4GalT5 morpholino results in mild dorsalization manifested by a slight tail coil. This phenotype is similar to the *pgy* phenotype reported by Mullins et al. (Mullins et al., 1996) and correlates with their Class 3. (Class 4) 10 ng of morpholino produces a more significant coiling of the tail, as well as dorsalization within the anterior regions of the embryo, and embryos are considered moderately dorsalized, similar to the *snh* phenotype representing Class 4 of Mullins et al. (Mullins et al., 1996). (Class 5) Injection of 15-20 ng of β4GalT5 morpholino produces the most severe dorsalization, which appears similar to that seen in the *swr* mutant. (**D**) Lateral view of 26-somite embryo injected with β4GalT5MO3 and mRNA encoding full-length β4GalT5. These embryos were essentially wild type in appearance. (**E**) In situ hybridization of *pax2a* in the otic vesicle of 26-somite control embryo; asterisks indicate the paired otoliths, which are absent in an equivalently staged β4GalT5MO embryo.

Smad activation is decreased in β4GalT5 morphants

Bmps affect gene expression through the activation of the Smad family of transcription factors. Bmp receptor activation leads to phosphorylation of the R-Smad proteins (receptor-regulated Smads1/5/8), which are subsequently released from the receptor and

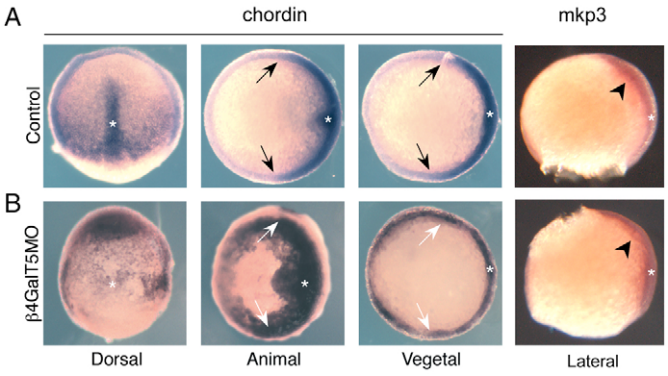

Fig. 4. Misexpression of *chordin* in β4GalT5MO embryos. (**A**) In situ hybridizations of *chordin* in control-injected embryos show that expression is restricted to the dorsal axis (asterisk in all panels). Arrows indicate the limits of *chordin* expression and identify the presumptive dorsoventral boundary. (**B**) Embryos injected with β4GalT5MO display disorganized *chordin* expression, including invasion into the presumptive ventral domain. For comparison, the limits of *chordin* expression in control embryos (A) are indicated by the white arrows. In β4GalT5 morphants, *chordin* expression extends beyond the boundaries seen in control embryos and envelope the ventral hemisphere. In contrast to that seen with chordin, the expression of the Fgf target *mkp3* (arrowheads) appears unaffected in morpholino-injected embryos.

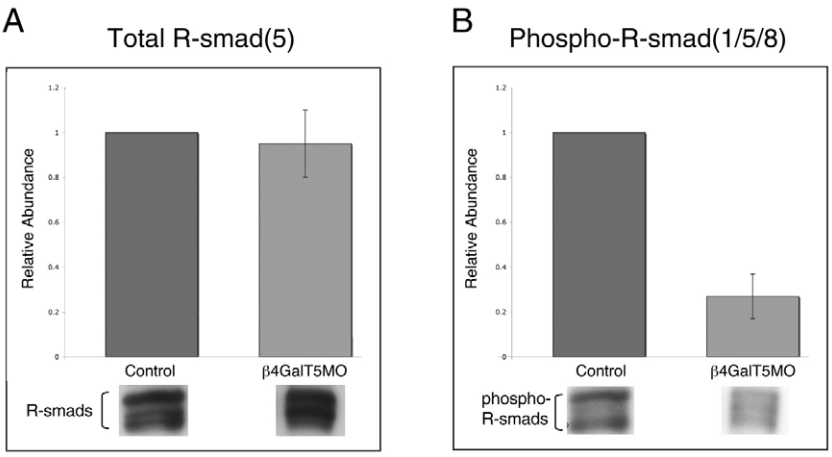

Fig. 5. Inefficient activation of Smad proteins in β4GalT5MO embryos. (**A**,**B**) Epiboly stage embryos were lyzed and assayed for (A) total or (B) activated Smad proteins by western immunoblotting, which was scanned and quantified. Levels of R-Smads (assayed using an anti-Smad5 antibody) and phospho-R-Smads (assayed using anti-phospho Smads1/5/8) were normalized to total protein loads. Expression is presented relative to control levels. No difference in the levels of total R-Smads was detectable between control-injected and β4GalT5MO-injected embryos, although activation of the Smad1/5/8 complex was reduced by 73% in β4GalT5MO embryos. Similar results were obtained in three separate experiments using both translation-blocking and splice-blocking morpholino oligonucleotides. Error bars indicate s.e.m.

form a heteromeric complex with the common Smad, Smad4. The phosphorylated R-Smad/Smad4 complex is translocated into the nucleus, where it regulates gene transcription (Mehra and Wrana, 2002).

During dorsoventral patterning, Bmp2b signaling results in the phosphorylation of Smad5 (and possibly Smad1 and/or Smad8) (Wrana and Attisano, 2000), and, consequently, the levels of total and activated (i.e. phosphorylated) R-Smads were assayed in 80% epiboly embryos following injection of either control or β4GalT5 morpholinos (Fig. 5). Whereas the total level of R-Smad5 (and other R-Smads as well) was similar in control and β4GalT5MO embryos (Fig. 5A), the level of phosphorylated R-Smads in β4GalT5MO embryos was only 27% of control levels (Fig. 5B), indicating a severe reduction in the activation of the Bmp signaling pathway. Similar results were obtained using β4GalT5MO embryos injected with either splice blocking or translation blocking oligonucleotides. We next examined the basis whereby a defect in β4GalT5-dependent glycosylation alters the activation of Bmp-dependent Smad proteins.

Reduced glycosylation of high molecular weight proteoglycans in β4GalT5 morphant embryos

It has become clear during the past few years that the ability of soluble cytokines to maintain stable expression domains is dependent upon their binding to the glycosaminoglycan (GAG) chains of large molecular weight proteoglycans. However, virtually all of our knowledge comes from the study of specific cytokines, such as Egf and Fgf, which bind to defined pentasaccharide structures within the heparan sulfate chains of proteoglycans (Hardingham and Fosang, 1992; Norton et al., 2005). Although other cytokines, including members of the Tgfβ superfamily to which the Bmps belong, have also been shown to bind proteoglycan GAG chains, the overall binding specificity of proteoglycans for these other cytokines has yet to be demonstrated. As we have no evidence to suggest that the expression of either *bmp2b* or *bmp7* is altered, we examined whether the defective Bmp signaling characteristic of β4GalT5MO embryos can be attributed to abnormal proteoglycan biosynthesis.

Initially, proteoglycans were isolated from both wild-type and β4GalT5MO embryos. On average, each wild-type embryo produced 18.3 ng of proteoglycans; whereas, only 4.8 ng were isolated from a typical β4GalT5MO embryo. Similar results were found using three independent proteoglycan isolations. To determine whether this reduction in proteoglycan mass was associated with alterations in protein and/or carbohydrate content, the proteoglycan preparation was resolved by SDS-PAGE under non-reducing conditions and stained for both protein and carbohydrate. Two prominent bands were apparent with relative molecular mass of >400 kDa and ~300 kDa, both of which contained similar protein levels in control and β4GalT5MO preparations (Fig. 6A). Both polypeptide species were highly glycosylated in the control sample (Fig. 6A); however, the same polypeptide bands showed dramatically less carbohydrate content in the β4GalT5MO sample (Fig. 6A). Thus, the proteoglycan core proteins appear to be

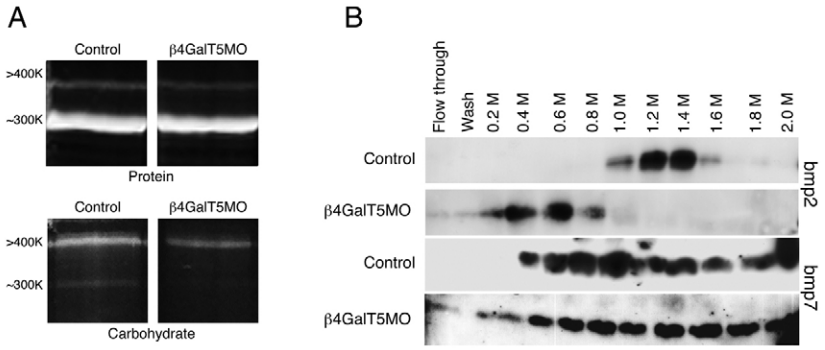

Fig. 6. Decreased binding of BMP2 to β4GalT5MO proteoglycans. (**A**) Proteoglycans isolated from control- and β4GalT5MO-injected embryos were resolved by 6% SDS-PAGE into two high molecular weight bands. Protein and carbohydrate content were revealed by staining with SPYRO and Pro-Q Emerald, respectively. Protein levels in each molecular weight species appear similar between control and β4GalT5MO samples, whereas the extent of glycosylation is dramatically reduced in β4GalT5MO embryos. (**B**) Proteoglycans from control-injected or β4GalT5MO-injected embryos were bound to an affinity support and assayed for their ability to bind recombinant BMP2 and BMP7. BMP2 showed peak elution from control proteoglycans at 0.8-1.6 M NaCl. BMP2 eluted from β4GalT5MO proteoglycans at 0.2-0.8 M NaCl. Interestingly, there was no significant difference in the ability of control or β4GalT5MO proteoglycans to bind recombinant BMP7. Similar results were obtained using proteoglycans isolated from embryos injected with either splice-blocking (MO2) or translation-blocking (MO3) oligonucleotides.

synthesized normally in β4GalT5MO embryos, but are grossly underglycosylated relative to those in control-injected embryos. Surprisingly, the underglycosylated proteoglycans from β4GalT5 morphants resolved at a similar molecular mass to control proteoglycans, suggesting either that the β4GalT5 deficiency does not lead to a global loss of GAG side-chains or that any reduction in molecular weight, given the relative amount of carbohydrate in the native proteoglycan, is too small to be resolved by the 6% SDS-polyacrylamide gel. In any event, the proteoglycans from β4GalT5 morphants show reduced glycosylation, and we therefore determined whether this influenced its ability to bind Bmp2 and/or Bmp7.

β4GalT5 morphant proteoglycans fail to bind recombinant BMP2

Proteoglycans were extracted from 80% epiboly stage embryos and coupled to an affinity support to which recombinant human BMP2 or BMP7 was applied, and any unbound protein was removed by washing. Bound BMP2 or BMP7 was eluted by increasing the salt concentration. BMP2 was eluted from control proteoglycans (Fig. 6B) at 0.8-1.6 M NaCl, similar to what others have shown for the binding of recombinant Noggin and Bmp4 to synthetic heparin sulfate (Paine-Saunders et al., 2002). When BMP2 was applied to proteoglycans isolated from β4GalT5MO embryos (Fig. 6B), BMP2 eluted from the column at 0.2 M NaCl and was completely eluted by 0.8 M NaCl. Similar results were obtained using proteoglycans isolated from β4GalT5MO embryos injected with either splice blocking (MO2) or translational blocking (MO3) oligonucleotides. This demonstrates that proteoglycans isolated from β4GalT5MO embryos show a reduced binding affinity for BMP2, relative to control proteoglycans.

We determined whether the decrease in BMP2 affinity to β4GalT5MO proteoglycans was specific to BMP2 or characteristic for other cytokines as well. As Bmp7 is the other major ventralizing agent in the late epiboly stage embryo, the affinity of BMP7 for control and β4GalT5MO proteoglycans was analyzed (Dick et al., 2000). BMP7 showed a distinctly different elution profile from that seen with BMP2, with a broad elution profile between 0.4-1.4 M NaCl (Fig. 6B). Unlike that seen with BMP2, BMP7 showed a similar elution pattern from proteoglycans isolated from both control-injected and β4GalT5MO embryos. This indicates that β4GalT5 generates a proteoglycan epitope that has apparent specificity for Bmp2, but not for Bmp7.

DISCUSSION

The results presented here represent the first functional characterization of a specific glycosyltransferase during early patterning of the zebrafish embryo. β4GalT5 was initially identified by an in silico search, and was subsequently cloned from a 48-hour RNA library. At the amino acid level, β4GalT5 is 69.9% identical to the human β4GalT5. β4GalT5 is not expressed in the oocyte, but is expressed by the early epiboly stage and reaches a steady state level of expression by mid-somitogenesis. Furthermore, β4GalT5 shows widespread expression throughout the embryo during the first 24 hours of development, with enhanced expression within several structures at the 20-somite stage. Insight into the biological function of β4GalT5 was addressed by the injection of three specific morpholino oligonucleotides, all of which resulted in a dorsalized embryo. Consistent with the hypothesis that β4GalT5 is essential for patterning of the dorsoventral axis, the expression of chordin was inappropriately expanded into the ventral hemisphere, similar to what is observed with well-studied dorsoventral patterning mutants (Miller-Bertoglio et al., 1997), thus suggesting that Bmp signaling was defective. This was confirmed by a dramatic reduction in the activation of the Bmp-dependent transcription factors Smad1/5/8. Because the trafficking and signaling efficacy of peptide cytokines are thought to be regulated by binding to GAG chains of proteoglycans, it is noteworthy that proteoglycans isolated from β4GalT5MO embryos demonstrated defective glycosylation and a greatly reduced affinity for Bmp2. These results suggest that β4GalT5 generates an epitope within the glycoside chains of proteoglycans that is required for proper Bmp signaling.

Previous analysis of glycosyltransferase function during development has relied upon generating knockouts of individual transferases or through random mutagenesis. Although these approaches have yielded insights into the function of a few specific glycosyltransferases, there is still a plethora of glycosyltransferases that remain uncharacterized (Bulik and Robbins, 2002; Furukawa et al., 2001; Lu et al., 1997; Maly et al., 1996; Wandall et al., 2005). Furthermore, because of the large number of glycosyltransferases now known to exist in mammalian tissues, and because of a poor understanding of the substrate specificity for each enzyme, it is difficult to accurately identify individual glycosyltransferases that are likely to be essential during development. For example, there are currently six confirmed β4GalTs in the mammalian genome, and this reflects just one arm of the larger glycosyltransferase ‘superfamily’ (Lowe, 1991). An initial search of the human genome suggests upwards of 300 glycosyltransferases are encoded. Generating targeted knockouts in all of these genes to identify those that have functions during development would be a monumental task.

Invertebrate systems have yielded new insight into developmentally essential glycosyltransferases. For example, in *C. elegans*, *sqv-3*, *sqv-7* and *sqv-8* predominantly affect the glycosylation of chondroitin sulfate and heparan sulfate proteoglycans (Bulik and Robbins, 2002). As a result of defective glycosylation, the vulval epithelium that normally invaginates to form a tube, is either collapsed or completely absent. Similarly, the *Drosophila* mutants *fringe*, *brainiac* and *egghead* all encode glycosyltransferases with important developmental roles. Fringe is a *N*-acetylgalactosaminyltransferase that is required for regulating Notch signaling by modulating its ligand-binding specificity (Moloney et al., 2000). *brainiac* and *egghead* are embryonic lethal mutations that encode glycosyltransferases required for the synthesis of the core carbohydrate in glycosphingolipids (Wandall et al., 2005).

Classically, glycosyltransferases are required for the posttranslational modification of virtually all membrane bound and secreted glycoproteins and glycolipids, so it is not surprising that β4GalT5 showed widespread expression throughout the embryo. Although the widespread expression of glycosyltransferases has made it difficult to determine which ones are likely to play crucial roles during embryogenesis, the power of zebrafish has allowed us to screen the knockdown phenotype of individual transferases to identify those that are essential during development. Through this approach, we have identified a β4GalT transcript that is required for dorsoventral patterning of the early embryo, but which had no precedent for having a role in vertebrate or invertebrate embryogenesis.

Specification of the dorsoventral axis is dependent upon Bmp signaling, as shown by mutations in *swirl/bmp2b*, *snailhouse/bmp7* and *somitabun/smad5* (Dick et al., 2000; Hild et al., 1999; Nguyen et al., 1998). At the onset of gastrulation, Bmps are present throughout the embryo, and not until the initial stages of dorsoventral patterning do Fgf8, Bozozok, and possibly members of the Wnt family repress Bmp signaling in the presumptive dorsal

region of the embryo (Furthauer et al., 2004; Kishimoto et al., 1997; Solnica-Krezel and Driever, 2001). Once the dorsal organizer has been established, Chordin, Follistatin and Noggin repress Bmp signaling by physically inhibiting the binding of Bmp to its receptor (Iemura et al., 1998; Piccolo et al., 1996; Zimmerman et al., 1996). A feedback loop is established whereby Bmp2b/Bmp7 inhibit Chordin through the activation of a chordin-specific protease, Tolloid (Blader et al., 1997). Upon Bmp receptor activation, the R-Smad proteins (e.g. Smad5) are phosphorylated and released from the receptor complex to form heteromeric complexes with Smad4; these heteromeric complexes then translocate to the nucleus where they activate the transcription of genes that direct ventralization (Kimelman and Pyati, 2005; Mehra and Wrana, 2002; O'Connor et al., 2006; Padgett et al., 1998).

Defective Bmp signaling leads to the inappropriate expansion of chordin expression into the presumptive ventral domain. In this study, we observed a similar expansion of chordin expression, suggesting a reduction of Bmp signaling in β4GalT5MO embryos. Furthermore, we determined that the activated Smad signaling complex was inefficiently activated in β4GalT5MO embryos, thus confirming a reduction in Bmp signaling. In order to determine how defective galactosylation in β4GalT5MO embryos could affect Bmp-dependent signaling pathways, we compared proteoglycans from control and β4GalTMO embryos, as proteoglycans are known to regulate cytokine binding and trafficking across the epithelial sheet.

Proteoglycans are a diverse class of extracellular proteins that consist of a protein core anchored to the plasma membrane by either a transmembrane domain (syndecans) or by a glycosylphosphatidylinositol (GPI) anchor (glypicans); some proteoglycans can be secreted as well (perlecans) (Kreis and Vale, 1999). Attached to the core protein are multiple, large molecular weight GAG chains that account for as much as 90% of the proteoglycan mass, and which contain a linker region followed by a repeating disaccharide unit unique to each GAG type (Sugahara and Kitagawa, 2000). GAG chains can be further modified by the addition of sulfate groups to specific monosaccharide residues (Chapman et al., 2004), and there is some evidence to suggest that the position of sulfate groups along the GAG chain directs cytokine binding. Knockdown of a specific sulfotransferase in zebrafish, zHS6ST, results in a phenotype similar to *knypek*, which encodes a glypican involved in non-canonical Wnt signaling, thus suggesting a role for GAG chains in the modulation of Wnt signaling (Bink et al., 2003; Topczewski et al., 2001). However, the *Drosophila* homolog of zHS6ST, dHS6ST, is not involved in Wnt signaling, although dHS6ST participates in Fgf signaling (Kamimura et al., 2001). Although these studies suggest that sulfation can be crucial to ligand binding, it is still unclear how alterations in sulfation directly regulate ligand specificity. Our work suggests that carbohydrate moieties outside of the traditional GAG chain and independent of sulfation can impact ligand-binding specificity as well.

Of all of the proteoglycans, the most intensely studied are those that contain heparan sulfate GAG chains. *dally* is a *Drosophila* heparan sulfate proteoglycan that has been shown to interact with *dpp* (a member of the Tgfβ family of cytokines that includes the Bmps) in the *Drosophila* imaginal disk (Jackson et al., 1997). *Dally* is also required for *wingless* (*wg*) signaling in the wing disc by interacting with the Wg receptor, Frizzled 2 (Cadigan et al., 1998). However, there is no evidence that *dally* interacts with *dpp* during embryogenesis, where *dpp* is essential for dorsoventral axis patterning.

We interpret the results presented here to suggest that β4GalT5 participates in the synthesis of oligosaccharide chains of zebrafish proteoglycans that are essential for Bmp2 binding and subsequent presentation to its receptor, thus triggering Smad activation. β4GalT5 has no apparent role in the synthesis or expression of Bmp2, only in its ability to bind and/or activate its receptor. Consequently, injection of recombinant Bmp2, or its mRNA, would not be expected to rescue the morphant phenotype unless one could bypass the requirement for proteoglycans and insure that Bmp2 was presented to its receptor with equal efficacy as wild type. In a similar study, defective synthesis of heparan sulfate proteoglycans that leads to reduced Fgf10 signaling could not be rescued by the injection of Fgf10 protein (Norton et al., 2005).

It is interesting that whereas proteoglycans isolated from β4GalT5MO embryos show reduced affinity for Bmp2, relative to control proteoglycans, binding of the closely related cytokine Bmp7 was relatively unaffected. The structure of the β4GalT5 epitope involved in Bmp2 binding is of obvious interest, but because the substrate specificity of the β4GalT5 identified here remains unknown, identification must await structural analysis of the relevant proteoglycan chains. In any event, this is the first report in which the ligand binding affinity of an endogenous proteoglycan can be modulated by a specific β1,4-galactosylation. Furthermore, these results raise the possibility that the ligand-binding specificity of proteoglycans may be defined by a carbohydrate 'code' involving glycoside residues both internal and external to the traditional GAG chains.

The authors thank Drs Win Sale, Karl Saxe and Iain Shepherd for suggestions regarding the manuscript. This work was supported by grant RO1 DE07120 from the NIH to B.D.S. and A.F.

References

Bink, R. J., Habuchi, H., Lele, Z., Dolk, E., Joore, J., Rauch, G. J., Geisler, R., Wilson, S. W., den Hertog, J., Kimata, K. et al. (2003). Heparan sulfate 6-o-sulfotransferase is essential for muscle development in zebrafish. *J. Biol. Chem.* **278**, 31118-31127.

Blader, P., Rastegar, S., Fischer, N. and Strahle, U. (1997). Cleavage of the BMP-4 antagonist chordin by zebrafish tolloid. *Science* **278**, 1937-1940.

Bulik, D. A. and Robbins, P. W. (2002). The Caenorhabditis elegans sqv genes and functions of proteoglycans in development. *Biochim. Biophys. Acta* **1573**, 247-257.

Cadigan, K. M., Fish, M. P., Rulifson, E. J. and Nusse, R. (1998). Wingless repression of Drosophila frizzled 2 expression shapes the Wingless morphogen gradient in the wing. *Cell* **93**, 767-777.

Chapman, E., Best, M. D., Hanson, S. R. and Wong, C. H. (2004). Sulfotransferases: structure, mechanism, biological activity, inhibition, and synthetic utility. *Angew. Chem. Int. Ed. Engl.* **43**, 3526-3548.

Dick, A., Hild, M., Bauer, H., Imai, Y., Maifeld, H., Schier, A. F., Talbot, W. S., Bouwmeester, T. and Hammerschmidt, M. (2000). Essential role of Bmp7 (snailhouse) and its prodomain in dorsoventral patterning of the zebrafish embryo. *Development* **127**, 343-354.

Domino, S. E., Zhang, L., Gillespie, P. J., Saunders, T. L. and Lowe, J. B. (2001). Deficiency of reproductive tract alpha(1,2)fucosylated glycans and normal fertility in mice with targeted deletions of the FUT1 or FUT2 alpha(1,2)fucosyltransferase locus. *Mol. Cell. Biol.* **21**, 8336-8345.

Furthauer, M., Van Celst, J., Thisse, C. and Thisse, B. (2004). Fgf signalling controls the dorsoventral patterning of the zebrafish embryo. *Development* **131**, 2853-2864.

Furukawa, K., Takamiya, K., Okada, M., Inoue, M., Fukumoto, S. and Furukawa, K. (2001). Novel functions of complex carbohydrates elucidated by the mutant mice of glycosyltransferase genes. *Biochim. Biophys. Acta* **1525**, 1-12.

Hagen, F. K., Hazes, B., Raffo, R., deSa, D. and Tabak, L. A. (1999). Structure-function analysis of the UDP-N-acetyl-D-galactosamine:polypeptide N-acetylgalactosaminyltransferase. Essential residues lie in a predicted active site cleft resembling a lactose repressor fold. *J. Biol. Chem.* **274**, 6797-6803.

Hardingham, T. E. and Fosang, A. J. (1992). Proteoglycans: many forms and many functions. *FASEB J.* **6**, 861-870.

Hascall, V. C. and Kimura, J. H. (1982). Proteoglycans: isolation and characterization. *Methods Enzymol.* **82**, 769-800.

Hild, M., Dick, A., Rauch, G. J., Meier, A., Bouwmeester, T., Haffter, P. and

Hammerschmidt, M. (1999). The smad5 mutation somitabun blocks Bmp2b signaling during early dorsoventral patterning of the zebrafish embryo. *Development* **126**, 2149-2159.
Iemura, S., Yamamoto, T. S., Takagi, C., Uchiyama, H., Natsume, T., Shimasaki, S., Sugino, H. and Ueno, N. (1998). Direct binding of follistatin to a complex of bone-morphogenetic protein and its receptor inhibits ventral and epidermal cell fates in early Xenopus embryo. *Proc. Natl. Acad. Sci. USA* **95**, 9337-9342.
Ioffe, E. and Stanley, P. (1994). Mice lacking N-acetylglucosaminyltransferase I activity die at mid-gestation, revealing an essential role for complex or hybrid N-linked carbohydrates. *Proc. Natl. Acad. Sci. USA* **91**, 728-732.
Jackson, S. M., Nakato, H., Sugiura, M., Jannuzi, A., Oakes, R., Kaluza, V., Golden, C. and Selleck, S. B. (1997). dally, a Drosophila glypican, controls cellular responses to the TGF-beta-related morphogen, Dpp. *Development* **124**, 4113-4120.
Kamimura, K., Fujise, M., Villa, F., Izumi, S., Habuchi, H., Kimata, K. and Nakato, H. (2001). Drosophila heparan sulfate 6-O-sulfotransferase (dHS6ST) gene. Structure, expression, and function in the formation of the tracheal system. *J. Biol. Chem.* **276**, 17014-17021.
Kimelman, D. and Pyati, U. J. (2005). Bmp signaling: turning a half into a whole. *Cell* **123**, 982-984.
Kimmel, C. B., Ballard, W. W., Kimmel, S. R., Ullmann, B. and Schilling, T. F. (1995). Stages of embryonic development of the zebrafish. *Dev. Dyn.* **203**, 253-310.
Kishimoto, Y., Lee, K. H., Zon, L., Hammerschmidt, M. and Schulte-Merker, S. (1997). The molecular nature of zebrafish swirl: BMP2 function is essential during early dorsoventral patterning. *Development* **124**, 4457-4466.
Kreis, T. and Vale, R. (1999). *Guidebook to the Extracellular Matrix, Anchor, and Adhesion Proteins*. Oxford, New York: Oxford University Press.
Lo, N. W., Shaper, J. H., Pevsner, J. and Shaper, N. L. (1998). The expanding beta 4-galactosyltransferase gene family: messages from the databanks. *Glycobiology* **8**, 517-526.
Lowe, J. B. (1991). Molecular cloning, expression, and uses of mammalian glycosyltransferases. *Semin. Cell Biol.* **2**, 289-307.
Lu, Q., Hasty, P. and Shur, B. D. (1997). Targeted mutation in beta1,4-galactosyltransferase leads to pituitary insufficiency and neonatal lethality. *Dev. Biol.* **181**, 257-267.
Maly, P., Thall, A., Petryniak, B., Rogers, C. E., Smith, P. L., Marks, R. M., Kelly, R. J., Gersten, K. M., Cheng, G., Saunders, T. L. et al. (1996). The alpha(1,3)fucosyltransferase Fuc-TVII controls leukocyte trafficking through an essential role in L-, E-, and P-selectin ligand biosynthesis. *Cell* **86**, 643-653.
Mehra, A. and Wrana, J. L. (2002). TGF-beta and the Smad signal transduction pathway. *Biochem. Cell Biol.* **80**, 605-622.
Miller-Bertoglio, V. E., Fisher, S., Sanchez, A., Mullins, M. C. and Halpern, M. E. (1997). Differential regulation of chordin expression domains in mutant zebrafish. *Dev. Biol.* **192**, 537-550.
Moloney, D. J., Panin, V. M., Johnston, S. H., Chen, J., Shao, L., Wilson, R., Wang, Y., Stanley, P., Irvine, K. D., Haltiwanger, R. S. et al. (2000). Fringe is a glycosyltransferase that modifies Notch. *Nature* **406**, 369-375.
Mullins, M. C., Hammerschmidt, M., Kane, D. A., Odenthal, J., Brand, M., van Eeden, F. J., Furutani-Seiki, M., Granato, M., Haffter, P., Heisenberg, C. P. et al. (1996). Genes establishing dorsoventral pattern formation in the zebrafish embryo: the ventral specifying genes. *Development* **123**, 81-89.
Nasevicius, A. and Ekker, S. C. (2000). Effective targeted gene 'knockdown' in zebrafish. *Nat. Genet.* **26**, 216-220.
Nechiporuk, A., Linbo, T. and Raible, D. W. (2005). Endoderm-derived Fgf3 is necessary and sufficient for inducing neurogenesis in the epibranchial placodes in zebrafish. *Development* **132**, 3717-3730.
Nguyen, V. H., Schmid, B., Trout, J., Connors, S. A., Ekker, M. and Mullins, M. C. (1998). Ventral and lateral regions of the zebrafish gastrula, including the neural crest progenitors, are established by a bmp2b/swirl pathway of genes. *Dev. Biol.* **199**, 93-110.
Norton, W. H. J., Ledin, J., Grandel, H. and Neumann, C. J. (2005). HSPG synthesis by zebrafish Ext2 and Ext13 is required for Fgf10 signaling during limb development. *Development* **132**, 4963-4973.
O'Connor, M. B., Umulis, D., Othmer, H. G. and Blair, S. S. (2006). Shaping BMP morphogen gradients in the Drosophila embryo and pupal wing. *Development* **133**, 183-193.
Padgett, R. W., Das, P. and Krishna, S. (1998). TGF-beta signaling, Smads, and tumor suppressors. *BioEssays* **20**, 382-390.
Paine-Saunders, S., Viviano, B. L., Economides, A. N. and Saunders, S. (2002). Heparan sulfate proteoglycans retain Noggin at the cell surface: a potential mechanism for shaping bone morphogenetic protein gradients. *J. Biol. Chem.* **277**, 2089-2096.
Pfeffer, P. L., Gerster, T., Lun, K., Brand, M. and Busslinger, M. (1998). Characterization of three novel members of the zebrafish Pax2/5/8 family: dependency of Pax5 and Pax8 expression on the Pax2.1 (noi) function. *Development* **125**, 3063-3074.
Piccolo, S., Sasai, Y., Lu, B. and De Robertis, E. M. (1996). Dorsoventral patterning in Xenopus: inhibition of ventral signals by direct binding of chordin to BMP-4. *Cell* **86**, 589-598.
Solnica-Krezel, L. and Driever, W. (2001). The role of the homeodomain protein Bozozok in zebrafish axis formation. *Int. J. Dev. Biol.* **45**, 299-310.
Sugahara, K. and Kitagawa, H. (2000). Recent advances in the study of the biosynthesis and functions of sulfated glycosaminoglycans. *Curr. Opin. Struct. Biol.* **10**, 518-527.
Suzuki, H., Maegawa, S., Nishibu, T., Sugiyama, T., Yasuda, K. and Inoue, K. (2000). Vegetal localization of the maternal mRNA encoding an EDEN-BP/Bruno-like protein in zebrafish. *Mech. Dev.* **93**, 205-209.
Thisse, C. and Thisse, B. (1998). High resolution whole-mount in situ hybridization. In *The Zebrafish Science Monitor*. Vol. 5 (ed. M. Westerfield), pp. 8-9. Eugene, OR: ZFIN.
Thompson, J. D., Higgins, D. G. and Gibson, T. J. (1994). CLUSTAL W: improving the sensitivity of progressive multiple sequence alignment through sequence weighting, position-specific gap penalties and weight matrix choice. *Nucleic Acids Res.* **22**, 4673-4680.
Topczewski, J., Sepich, D. S., Myers, D. C., Walker, C., Amores, A., Lele, Z., Hammerschmidt, M., Postlethwait, J. and Solnica-Krezel, L. (2001). The zebrafish glypican knypek controls cell polarity during gastrulation movements of convergent extension. *Dev. Cell* **1**, 251-264.
Tsang, M., Maegawa, S., Kiang, A., Habas, R., Weinberg, E. and Dawid, I. B. (2004). A role for MKP3 in axial patterning of the zebrafish embryo. *Development* **131**, 2769-2779.
Varki, A. (1993). Biological roles of oligosaccharides: all of the theories are correct. *Glycobiology* **3**, 97-130.
Wandall, H. H., Pizette, S., Pedersen, J. W., Eichert, H., Levery, S. B., Mandel, U., Cohen, S. M. and Clausen, H. (2005). Egghead and brainiac are essential for glycosphingolipid biosynthesis in vivo. *J. Biol. Chem.* **280**, 4858-4863.
Westerfield, M. (1993). *The Zebrafish Book: A Guide for the Laboratory use of Zebrafish (Brachydanio rerio)*. Eugene, OR: M. Westerfield.
Wrana, J. L. and Attisano, L. (2000). The Smad pathway. *Cytokine Growth Factor Rev.* **11**, 5-13.
Yan, Y.-L., Willoughby, J., Liu, D., Crump, J. G., Wilson, C., Miller, C. T., Singer, A., Kimmel, C., Westerfield, M. and Postlethwait, J. H. (2005). A pair of Sox: distinct and overlapping functions of zebrafish sox9 co-orthologs in craniofacial and pectoral fin development. *Development* **132**, 1069-1083.
Zimmerman, L. B., De Jesus-Escobar, J. M. and Harland, R. M. (1996). The Spemann organizer signal noggin binds and inactivates bone morphogenetic protein 4. *Cell* **86**, 599-606.